


# Robust Fault Detection Scheme for Asynchronous Switched Systems via Sliding Mode Observer

Shafqat Ali, Yuchen Jiang\*, Hao Luo\*, Muhammad Taskeen Raza, Shah Faisal, and Faizan Shahid

**Abstract:** This work studies the fault detection problem for continuous-time asynchronous switched systems. For residual signal generation, we design a fault detection sliding mode observer such that residual characterizes the fault sensitivity level by  $H_-$  performance, and its robustness to process disturbance is determined by  $H_\infty$  performance. Specifically, the challenge entails addressing the phenomenon of asynchronous switching between the controlled object and the observer, where there is a delay between the switching of the subsystems and the observer. A piece-wise Lyapunov function and average dwell time approach are applied to resolve the asynchronous switching stability within matched and unmatched periods. A feasible solution is derived based on linear matrix inequalities. For effective fault detection, a residual evaluation scheme is provided with a threshold. Finally, simulation results on a buck-boost converter are furnished to validate the usefulness of the proposed approach.

**Keywords:** Asynchronous switched systems, average dwell time, fault detection,  $H_-/H_\infty$  performance index, linear matrix inequality, sliding mode observer.

## 1. INTRODUCTION

Model-based fault diagnosis has gained increasing attention over the past decades [1-3]. In recent years, fault diagnosis and fault tolerant control (FTC) have received considerable attention in both data-driven and model-based methods of fault diagnosis [4,5]. To increase their performance, modern systems need to operate safely and reliably. Hence, several serious failures occur in engineering and industrial applications such as chemical, nuclear power stations, and aerospace. Therefore, fault detection (FD) has received significant importance in recent years to enhance system efficiency [6-9]. The problem of false alarms and missing detection in many practical applications are due to the coupling of faults, disturbances, control inputs, and even cyber attacks [10]. Hence, the FD system becomes fault sensitive and robust to process disturbance. Different optimization performance indices for FD problems have been recommended, such as  $H_-/H_\infty$  [11-13],  $H_2/H_2$ , and  $H_\infty/H_\infty$  [14,15]. In our research, we pay particular attention to  $H_-/H_\infty$ . The  $H_-$  index characterizes maximum sensitivity to a fault, whereas the  $H_\infty$  performance tries to minimize the impact of disturbances on residual signals.

Switched systems [16-18] are prominent in hybrid dynamical networks. Therefore, they have gained considerable attention due to their industrial and practical applications [19-22]. Switched systems are generally composed of subsystems that have switching rules associated with them. The most significant issue is the design of switching rules in switched systems. Thus, better performance can be achieved by choosing a proper switching rule. However, real switched systems exist with definite switching signals such as, state-dependent, time-dependent, memory-dependent, and arbitrary switching signals. To address switched system stability, the average dwell time (ADT) is used, often employing a time-dependent switching signal. ADT switching is a sort of restricted switching signal in which the number of switches is fixed. It is also generally known that the ADT method specifies a broader class of stable switching signals, with the extreme case being arbitrary switching. As a result, both theoretically and practically, analyzing the stability of switched systems using ADT is important.

Besides, the FD issue in switched systems is an active research area and has attracted many researchers to explore further challenges of fault diagnosis in switched systems. FD is investigated in [23] for discrete-time switch-

Manuscript received February 24, 2023; revised May 11, 2023; accepted June 4, 2023. Recommended by Associate Editor M. Chadli under the direction of Senior Editor Sangmoon Lee. This work was supported in part by Natural Science Foundation of Heilongjiang Province under Grant LH2022F024, National Natural Science Foundation of China under Grant 62203143, Heilongjiang Province Postdoctoral Foundation under Grant LBH-Z22130.

Shafqat Ali, Yuchen Jiang, Hao Luo, Shah Faisal, and Faizan Shahid are with the Control and Simulation Center, Harbin Institute of Technology, Harbin 150001, China (e-mails: {sali406, yc.jiang, hao.luo, faisal.cse}@hit.edu.cn, 21BF04096@stu.hit.edu.cn). Muhammad Taskeen Raza is with the Department of Electrical Engineering, Lahore College for Women University, Lahore 54000, Pakistan (e-mail: taskeen.raza@lcwu.edu.pk).

\* Corresponding authors.

ing systems. A switching rule with dwell time constraints is devised, so that the switched system is asymptotically stable and has better detection performance. The observer design of the FD problem in the switched system is examined in [24], making all modes unstable. A discretised Lyapunov function is designed in this case, and the switching signal is derived using the average dwell time approach, taking into account the instability induced by the unobservable condition. For DC-DC boost converters, effective fault detection and identification systems are observed in [25]. The basis of this work's strategy is the creation of a robust linear switch fault detection observer and a series of fault recognition observers. The simultaneous robust control and detection problems are described in [26] for the discrete-time switching system to meet control and detection goals. A switching law and output feedback-based controller/detectors are developed. The problem of FTC is tackled in [27] for discrete-time switched linear parameter varying (LPV) systems. The switching behavior among the system's subsystems is regulated by means of a general dwell time. The study in [28] investigates the utilization of the parity space approach to address the fault detection issue in switched linear systems that operate in discrete time, with consideration of the dwell time constraint.

However, the aforementioned research on FD problems of switched systems contains a default assumption of asynchronous switching between the subsystem and observer. It means that the subsystem and observer switch at the same time. However, in practical applications, it is essential to allow a certain amount of time to identify active subsystems and observer switching. In general, there are asynchronous switching phenomena between subsystems and observers. Here, asynchronous means lag in switching between subsystem and observer. There exist multiple approaches to analyze and regulate the phenomenon of asynchronous switching in dynamic systems. Hybrid modeling is a highly effective method that combines both continuous and discrete system models to accurately represent the system's behavior. This approach is particularly advantageous for modeling asynchronous switched systems, as it captures the system's dynamics in both modes. Another potent method to evaluate the stability of asynchronous switched systems is the multiple Lyapunov function method, which constructs multiple Lyapunov functions for each mode of the system, and uses them to assess the overall system's stability. The technique of switched observer design involves creating observers for each mode of the system, which can be beneficial in estimating the system's state during switching events. Additionally, the sliding mode control strategy is another effective approach to stabilize asynchronous switched systems, by designing a controller that directs the system's state onto a sliding surface, where its behavior can be controlled. Other methods for controlling asynchronous switched systems

include adaptive control, robust control, and model predictive control. More recently, the problem of asynchronous switching has gained much attention in FD research community [29,30]. However, FD in asynchronous switched systems needs to be studied more thoroughly. An FD and isolation filter for asynchronous switching systems is designed in [29]. A residual signal is generated in the presence of disturbance. An observer is designed in [30] using the piece-wise Lyapunov function for integrated FD and control under asynchronous switching. Here, the problem is solved by manipulating the ADT and  $H_\infty$  control design method. Using the  $H_-/H_\infty$  approach, authors of [31] examine the asynchronous switching scenario caused by state delay for the simultaneous FD and control problem. ADT and the performance index for linear switched time-delay systems with asynchronous switching are used to determine stability and FD. A class of nonlinear systems susceptible to time-varying unknown delays on states is proposed in [32] along with resilient, adaptive FD and diagnosis observer design. The LMI approach is used to determine the existence of faults. Furthermore, the Lyapunov stability theory is used to attain asymptotic stability. ADT with mode-dependent asynchronous switching is studied in [33] for the stability of switched linear parameter varying systems. The controller matched and mismatched periods corresponding to subsystem switching are computed here using MDADT and Lyapunov stability criteria. A robust fuzzy observer based on SMO is proposed in [34] for the uncertain Takagi-Sugeno (T-S) fuzzy model, with the aim of tackling the FDI problem. The asynchronous switching cases, together with continuous and discrete-time systems, were achieved properly by using a non-weighted  $l_2/L_2$  gain performance in [35]. The asynchronous switching issue for simultaneous FD and control is addressed in [36]. Also, robustness and sensitivity to fault are guaranteed by designing a switching law and FD control unit. To address the asynchronous switched model and provide stability and control of switching systems, persistent dwell time is used in [37]. Here firstly, the  $l_2$  gain and stability analysis for the switched system is derived. Furthermore, Lyapunov-like functions are used while switching between system mode and controller during the mismatched time. A robust admissibility criterion is established in [38] for uncertain switched systems through the utilization of a switched Lyapunov function and a strict LMIs formulation. Fault detection and isolation (FDI) is studied in [39] by utilizing ADT for switched systems in discrete-time cases. For a type of continuous-time switched Takagi-Sugeno (T-S) fuzzy systems [40], the phenomenon of asynchronous switching arises between event triggered instants. Meanwhile, this technique developed the non-weighted  $H_\infty$  and stability criteria for switched TS fuzzy systems utilizing MDADT switching. The problem of asynchronous  $l_1$  filtering is explored in [41] for a class of discrete-time switched positive systems.

Here, upper and lower-bound positive filters are meant to assure the positivity, stability, and non-weighted  $l_1$  gain of the associated filtering error systems. The presence of disturbances significantly impacts the effectiveness of a control system. The results on realistic and bounded disturbances are available in the literature, and their impact is minimized to improve the system's output. Utilizing adaptive SMO, a simultaneous FD in actuator and sensor in [42] is suggested for wind turbines. In this case, the variation in wind speed represents a realistic disturbance. The stirred tank heater model is proposed in [43] as a solution for intermittent FD with severe noise and unknown disturbances. A framework is suggested in [44] for a Roesser system using event-triggered fault diagnosis and bounded disturbance. A sliding mode multiple observer is developed in [45] utilizing multiple models for FDI of a nonlinear dynamical system, with the goal of estimating the system's state vector. Developing an accurate FD scheme for asynchronous switched systems is a challenging task due to the complexity of the switched system's behavior, which arises from the time-varying behavior of the subsystems and observers, leading to matched and unmatched periods. Furthermore, SMOs are susceptible to disturbances and measurement noise, potentially resulting in false alarms or missed detections that can undermine the FD system's dependability. Additionally, it is challenging to design an SMO that can track the system dynamics accurately because of the asynchronous switching phenomenon. Hence, based on the preceding discussion and references, we will broaden the scope of our work for SMO-based FD in complex asynchronous switching problems by a mixed  $H_-/H_\infty$  technique. However, the previous studies of the literature on asynchronous switching control have not sufficiently examined this issue. Fault detection sliding mode observer (FDSMO) is designed for both matched and unmatched periods of asynchronous switching and stability of the respective switched system is achieved by Lyapunov Krasovskii functional method. Also,  $H_-/H_\infty$  criteria is used to make the residual signal robust to disturbances and sensitive to faults.

This paper proposes an FD technique that considers continuous-time asynchronous switching and the ADT approach while applying the multiobjective  $H_-/H_\infty$  optimization index. The main contributions of the present research are concluded as

- 1) For the generation of the residual signal, fault detection sliding model observer (FDSMO) is proposed for asynchronous switching systems in the presence of a fault and disturbance.
- 2) To examine the stability of asynchronous switching systems, we choose the Lyapunov function for both matched and unmatched periods along with average dwell time, such that switched system achieve asymptotic stability.
- 3) A mixed  $H_-/H_\infty$  performance index is utilized to design a fault detection observer that achieves both sensitivity and robustness to fault and disturbance simultaneously in such a way that the influence of the fault on the residual is maximized and the impact of the disturbance is reduced.
- 4) The simulation results of a buck-boost converter circuit illustrate the appropriateness of the prospective method.

The remaining content of the paper is structured as follows: Section 2 presents the given problem. The derivations of the most significant results related to  $H_-/H_\infty$  performance and asynchronous switched system stability are obtained in Section 3. Section 4 demonstrates a simulation study. Finally, the conclusion is provided in Section 5.

**Notations:** Some notations are adopted in this paper. The Hermitian matrix is  $He(Z) = Z + Z^T$  where  $Z$  is a square matrix of appropriate dimension. Here  $Z^T$  is the transposed matrix. In addition, the positive and negative definite matrix is denoted by  $A > 0$  and  $A < 0$ , respectively. Symmetric elements within the matrix are denoted by the symbol  $*$ .  $0$  and  $I$  are zero and identity matrices, respectively.

## 2. PROBLEM FORMULATION

Switched systems with sensor fault can be described as follows:

$$\begin{cases} \dot{x}(t) = A_{\sigma(t)}x(t) + B_{\sigma(t)}u(t) + E_{d\sigma(t)}d(t), \\ y(t) = C_{\sigma(t)}x(t) + F_{d\sigma(t)}d(t) + f_s(t), \end{cases} \quad (1)$$

where  $x(t) \in R^n$  denotes the state vector,  $u(t) \in R^m$  and  $y(t) \in R^p$  are, respectively the control input and measurement output vectors,  $d(t) \in R^r$  represents disturbance vector and  $f_s(t) \in R^q$  is sensor fault vector.  $\sigma(t) \in \{1, 2, \dots, k\}$  is the continuous-time switching signal, specifically a piece-wise constant function, where  $k > 1$  is subsystems number involved. For  $\sigma(t) = i$ , matrices of the system are represented by  $A_i \in R^{n \times n}$ ,  $B_i \in R^{n \times m}$ ,  $C_i \in R^{p \times n}$ ,  $E_{di} \in R^{n \times r}$ , and  $F_{di} \in R^{p \times r}$ .

For the generation of residual signal, the specified SMO for FD is chosen as

$$\begin{cases} \dot{\hat{x}}(t) = A_{\hat{\sigma}(t)}\hat{x}(t) + B_{\hat{\sigma}(t)}u(t) + G_{\hat{\sigma}(t)}(e_{y(t)}) + \vartheta(t), \\ \hat{y}(t) = C_{\hat{\sigma}(t)}\hat{x}(t), \\ e_{y(t)} = y(t) - \hat{y}(t), \end{cases} \quad (2)$$

where  $\hat{x}(t) \in R^n$  and  $\hat{y}(t) \in R^p$  are state and output estimations respectively.  $e_{y(t)}$  is the output estimation error.  $G_{\hat{\sigma}(t)}$  and  $\vartheta(t)$  are respectively the observer gain and non-linear injection terms. The observer switching signal is  $\hat{\sigma}(t)$ . Fig. 1 shows the block diagram representation of switched system model and SMO model while taking

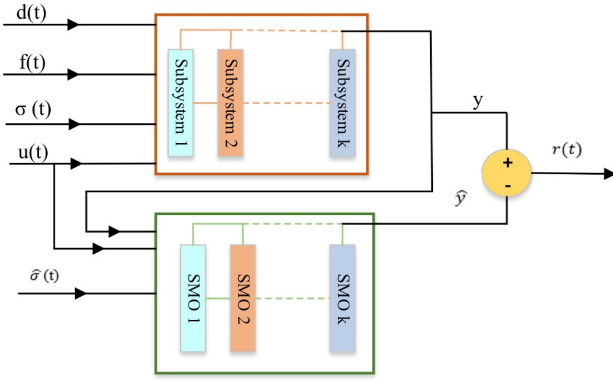


Fig. 1. The structure of switched system and asynchronously switching observers.

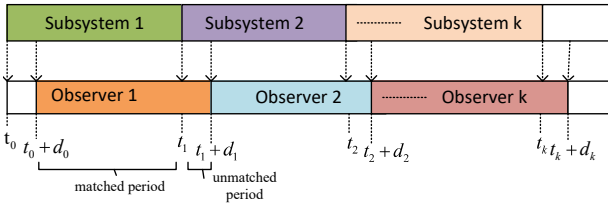


Fig. 2. Asynchronous switching between subsystem and observer.

asynchronous switching phenomena. In the presence of a disturbance  $d(t)$  and a fault  $f_s(t)$ , the switching system model is divided into  $k$  subsystems. The SMO model, on the other hand, is also divided into  $k$  number of observers as well. Subtracting the subsystem outputs  $y(t)$  from the observer outputs  $\hat{y}(t)$  yields the residual signal  $r(t)$ . Ideally, synchronous switching exist between subsystem and observer, that is,  $\sigma(t) = \hat{\sigma}(t) = i$ . But in practical applications, the observer takes considerable time for identification of the subsystem. Hence the asynchronous switching phenomenon arises. Here the observer lags behind the subsystem switching by a period of  $d_i$ , which is known a priori. Fig. 2 illustrates the asynchronous switching phenomenon between matched and unmatched periods. For any time duration  $t \in [t_{\mathbb{k}}, t_{\mathbb{k}+1})$ , where  $\mathbb{k} = 1, 2, 3, \dots$ , it follows that for any matched period where subsystem 1 and observer 1 are in operation, the interval is  $t \in [t_0, t_1) \cup [t_{\mathbb{k}-1} + d_{\mathbb{k}-1}, t_{\mathbb{k}})$ ,  $\mathbb{k} = 1, 2, 3, \dots$ , also for unmatched period there exist time duration  $t \in [t_{\mathbb{k}}, t_{\mathbb{k}} + d_{\mathbb{k}})$ ,  $\mathbb{k} = 1, 2, 3, \dots$ , where subsystem 2 and observer 1 are in operation.

The error dynamics  $\dot{e}(t)$  and residual signal  $r(t)$  for both matched and unmatched periods of asynchronous switching are described as

$$\begin{cases} \dot{e}(t) = (A_i - G_i C_i)e(t) + (E_{di} - G_i F_{di})d(t) \\ \quad - G_i f_s(t) - \vartheta_i(t), \\ r(t) = C_i e(t) + F_{di} d(t) + f_s(t), \end{cases} \quad (3)$$

$$\begin{cases} \dot{e}(t) = (A_i - G_i C_i)e(t) + (E_{dj} - G_i F_{dj})d(t) \\ \quad - G_i f_s(t) + (A_j - A_i + G_i C_i - G_i C_j)x(t) \\ \quad - \vartheta_{ij}(t), \\ r(t) = C_i e(t) + (C_j - C_i)x(t) + F_{dj}d(t) + f_s(t). \end{cases} \quad (4)$$

For optimal FD in switched systems that experience specific fault and disturbance,  $H_-/H_\infty$  performance index is utilized. This solution gives a sort of compromise between maximum sensitivity to fault and minimizes the disturbance to residual signal. To maintain the stability of asynchronous switched systems, the switching logic is generated using an ADT approach. The following are the key definitions that will be utilized to determine the solution to our desired approach.

**Definition 1 ( $H_-$  performance):** In order to ensure fault sensitivity to the residual signal and satisfy  $H_-$  performance, systems (3) and (4) must take into account zero initial conditions and disturbance  $d(t) = 0$ , if

$$\int_0^\infty r^T(s)r(s)ds \geq \beta^2 \int_0^\infty f_s^T(s)f_s(s)ds. \quad (5)$$

where  $\beta$  indicates the scalar parameter for fault sensitivity.

**Definition 2 ( $H_\infty$  performance):** Given that the attenuation constant parameter as  $\gamma$ , then systems (3) and (4) hold the robust  $H_\infty$  performance under zero initial conditions and fault  $f_s(t) = 0$ , if

$$\int_0^\infty r^T(s)r(s)ds \leq \gamma^2 \int_0^\infty d^T(s)d(s)ds. \quad (6)$$

**Definition 3 (Average dwell time) [16]:** Switching signal  $\sigma(t)$  satisfies ADT for any  $t_b \geq t_a \geq 0$  if we have

$$N_\sigma(\tau, t) \leq N_o + \frac{t_b - t_a}{\tau_a},$$

where  $\tau_a > 0$  is the ADT,  $N_\sigma(\tau, t)$  denotes the switching number over the period  $(t_a, t_b)$  and  $N_o \geq 0$  is the chattering bound which ensures that the system switches between subsystems smoothly and avoids undesirable chattering behavior.

**Remark 1:** In asynchronous switched systems, the ADT represents the minimum duration during which each subsystem must remain active before transitioning to another subsystem. This parameter plays a crucial role in determining the response characteristics of the switched system. Longer dwell times are associated with greater stability, while shorter dwell times can improve system responsiveness but also raise the risk of instability. Thus, our proposed method selects the ADT in asynchronous switched systems to ensure asymptotic stability while also enhancing system responsiveness.

### 3. MAIN RESULTS

This section formulates the FD problem as a multi-objective  $H_-/H_\infty$  problem, which is essentially a trade-off

with the maximum influence on fault sensitivity and the minimum influence on disturbance attenuation level to the residual signal. First, we analyse  $H_-$  optimization problem.

### 3.1. $H_-$ formulation

Consider the augmented form of systems (3) and (4) for both matched and unmatched periods. Assume that  $d(t) = 0$

$$\begin{cases} \dot{\mathfrak{J}}(t) = \bar{A}_i \mathfrak{J}(t) + \bar{B}_{fi} f_s(t) - \vartheta_i(t), \\ r(t) = \bar{C}_i \mathfrak{J}(t) + f_s(t), \end{cases} \quad (7)$$

$$\begin{cases} \dot{\mathfrak{J}}(t) = \bar{A}_{ij} \mathfrak{J}(t) + \bar{B}_{fij} f_s(t) - \vartheta_{ij}(t), \\ r(t) = \bar{C}_{ij} \mathfrak{J}(t) + f_s(t), \end{cases} \quad (8)$$

where  $\mathfrak{J}(t) = [x(t)^T \quad e(t)^T]^T$

$$\begin{cases} \bar{A}_i = \begin{bmatrix} A_i & 0 \\ 0 & A_i - G_i C_i \end{bmatrix}, \bar{B}_{fi} = \begin{bmatrix} 0 \\ -G_i \end{bmatrix}, \\ \bar{C}_i = [0 \quad C_i], \\ \bar{A}_{ij} = \begin{bmatrix} A_j & 0 \\ A_{12} & A_i - G_i C_i \end{bmatrix}, \\ A_{12} = A_j - A_i + G_i C_i - G_i C_j, \\ \bar{B}_{fij} = \begin{bmatrix} 0 \\ -G_i \end{bmatrix}, \bar{C}_{ij} = [C_j - C_i \quad C_i]. \end{cases}$$

**Lemma 1** [30]: Given scalars  $0 < \eta < 1$ ,  $0 < \wp < 1$ ,  $\beta > 0$ ,  $\mu_1 \geq 1$  and  $\mu_2 \geq 1$ , if the Lyapunov function candidates  $V_i(\mathfrak{J}(t))$  and  $V_{ij}(\mathfrak{J}(t))$  satisfying the following inequalities exist

$$\begin{aligned} V_j(\mathfrak{J}(t)) &\leq \mu_1 V_{ij}(\mathfrak{J}(t)), \\ V_{ij}(\mathfrak{J}(t)) &\leq \mu_2 V_i(\mathfrak{J}(t)), \\ \dot{V}_i(\mathfrak{J}(t)) &\leq -\eta V_i(\mathfrak{J}(t)) - \Upsilon_1, \\ \dot{V}_{ij}(\mathfrak{J}(t)) &\leq \wp V_{ij}(\mathfrak{J}(t)) - \Upsilon_1, \end{aligned}$$

where  $\Upsilon_1 = \beta^2 f_s^T(t) f_s(t) - r^T(t) r(t)$ , then the system achieves global asymptotic stability and has  $H_-$  performance along with ADT

$$\begin{aligned} \tau_a > \tau_a^* &= \frac{\ln(\mu_1 \mu_2)}{\xi^*}, \\ \frac{T^-(t_0, t)}{T^+(t_0, t)} &\geq \frac{\wp + \xi^*}{\eta - \xi^*}, \quad 0 < \xi^* < \eta. \end{aligned} \quad (9)$$

**Theorem 1:** For any given positive scalars  $0 < \eta < 1$ ,  $\wp > 0$ ,  $\beta > 0$ ,  $a_1 > 1$  and  $a_2 > 1$  then switched system (1) and fault detection sliding mode observer (2) satisfy global asymptotic stability and achieve  $H_-$  performance index (5) and switching signal besides ADT (9), provided that there exist positive definite symmetric matrices  $P_{s,i} > 0$ ,  $P_{s,ij} > 0$ ,  $Z_{s,i1} > 0$ ,  $Z_{s,ij1} > 0$ ,  $Z_{s,i2} > 0$  and  $Z_{s,ij2} > 0$ , such that the following inequalities hold.

$$\begin{bmatrix} -He(Z_{s,i1}) & \nabla & Z_{s,i1}^T \bar{B}_{fi} \\ * & \nabla_{he} + \nabla'' & \nabla_1 \\ * & * & \beta^2 I - I \end{bmatrix} \leq 0, \quad (10)$$

$$\begin{bmatrix} -He(Z_{s,ij1}) & \nabla_2 & Z_{s,ij1}^T \bar{B}_{fij} \\ * & \nabla'_{he} + \nabla'_3 & \nabla_4 \\ * & * & \beta^2 I - I \end{bmatrix} \leq 0, \quad (11)$$

where  $\nabla = P_{s,i} - a_1 Z_{s,i1} + Z_{s,i1}^T \bar{A}_i$ ,  $\nabla_{he} = He(Z_{s,i1}^T \bar{A}_i) a_1$ ,  $\nabla'' = -\bar{C}_i^T \bar{C}_i + \alpha P_{s,i}$ ,  $\nabla_1 = -\bar{C}_i^T + a_1 Z_{s,i1}^T \bar{B}_{fi}$ ,  $\nabla_2 = P_{s,ij} - a_2 Z_{s,ij1} + Z_{s,ij1}^T \bar{A}_{ij}$ ,  $\nabla'_{he} = He(Z_{s,ij1}^T \bar{A}_{ij}) a_2$ ,  $\nabla'_3 = -\bar{C}_{ij}^T \bar{C}_{ij} - \wp P_{s,ij}$  and  $\nabla_4 = -\bar{C}_{ij}^T + a_2 Z_{s,ij1}^T \bar{B}_{fij}$ .

**Proof:** Considering the Lyapunov-Krasovskii function for augmented systems (7) and (8) during both matched and unmatched periods.

$$V_a(\mathfrak{J}(t)) = \begin{cases} V_i(\mathfrak{J}(t)), & t \in [t_{k-1} + d_{k-1}, t_k), \\ V_{ij}(\mathfrak{J}(t)), & t \in [t_k, t_k + d_k). \end{cases}$$

We construct the Lyapunov function  $V_i(\mathfrak{J}(t))$  for the matched period and  $V_{ij}(\mathfrak{J}(t))$  for the mismatched period to ensure the stability of an asynchronous switched switching system. This can be stated as

$$\begin{cases} V_i(\mathfrak{J}(t)) = \mathfrak{J}^T(t) P_{s,i} \mathfrak{J}(t), \\ V_{ij}(\mathfrak{J}(t)) = \mathfrak{J}^T(t) P_{s,ij} \mathfrak{J}(t). \end{cases}$$

First, the Lyapunov function is modified for the matched period as

$$V_i(\mathfrak{J}(t)) = \mathfrak{J}^T(t) P_{s,i} \mathfrak{J}(t). \quad (12)$$

Differentiating the above equation throughout system (7) trajectory indicates

$$\dot{V}_i(\mathfrak{J}(t)) = \dot{\mathfrak{J}}^T(t) P_{s,i} \mathfrak{J}(t) + \mathfrak{J}^T(t) P_{s,i} \dot{\mathfrak{J}}(t). \quad (13)$$

Lemma 1 is modified for matched period as

$$\dot{V}_i(\mathfrak{J}(t)) + \eta V_i(\mathfrak{J}(t)) - r^T(t) r(t) + \beta^2 f_s^T(t) f_s(t) \leq 0. \quad (14)$$

Now the inequality is obtained by substituting (12), (13) and  $r(t)$  from (7) in (14) solve as

$$\begin{aligned} &\dot{\mathfrak{J}}^T(t) P_{s,i} \mathfrak{J}(t) + \mathfrak{J}^T(t) P_{s,i} \dot{\mathfrak{J}}(t) + \eta \mathfrak{J}^T(t) P_{s,i} \mathfrak{J}(t) \\ &+ \beta^2 f_s^T(t) f_s(t) - [\bar{C}_i \mathfrak{J}(t) + f_s(t)]^T \\ &\times [\bar{C}_i \mathfrak{J}(t) + f_s(t)] \leq 0. \end{aligned} \quad (15)$$

After substituting  $\dot{\mathfrak{J}}(t)$  from (7) into (15), the above inequality can be easily written as follows:

$$\begin{aligned} &\dot{\mathfrak{J}}^T(t) \bar{A}_i^T P_{s,i} \mathfrak{J}(t) + f_s^T(t) \bar{B}_{fi}^T P_{s,i} \mathfrak{J}(t) + \mathfrak{J}^T(t) P_{s,i} \bar{A}_i \mathfrak{J}(t) \\ &+ \mathfrak{J}^T(t) P_{s,i} \bar{B}_{fi} f_s(t) + \eta \mathfrak{J}^T(t) P_{s,i} \mathfrak{J}(t) \\ &- \mathfrak{J}^T(t) \bar{C}_i^T \bar{C}_i \mathfrak{J}(t) - \mathfrak{J}^T(t) \bar{C}_i^T f_s(t) - f_s^T(t) \bar{C}_i \mathfrak{J}(t) \\ &- f_s^T(t) f_s(t) + \beta^2 f_s^T(t) f_s(t) - 2\eta \|\mathfrak{J}(t)\| \leq 0. \end{aligned} \quad (16)$$

Thus (16) is expressed in such a way as

$$\begin{bmatrix} \mathfrak{J}^T(t) & f_s^T(t) \end{bmatrix} H \begin{bmatrix} \mathfrak{J}(t) \\ f_s(t) \end{bmatrix} \leq 0. \quad (17)$$

Here,

$$H = \begin{bmatrix} \Theta_h & P_{s,i} \bar{B}_{fi} - \bar{C}_i^T \\ * & \beta^2 I - I \end{bmatrix}, \quad (18)$$

where  $\Theta_h = \bar{A}_i^T P_{s,i} + P_{s,i} \bar{A}_i + \eta P_{s,i} - \bar{C}_i^T \bar{C}_i$ . Also rewrite (18) as

$$\begin{bmatrix} \bar{A}_i^T & I & 0 \\ \bar{B}_{fi} & 0 & I \end{bmatrix} \Pi \begin{bmatrix} \bar{A}_i & \bar{B}_{fi} \\ I & 0 \\ 0 & I \end{bmatrix} < 0, \quad (19)$$

where

$$\Pi = \begin{bmatrix} 0 & P_{s,i} & 0 \\ P_{s,i} & -\bar{C}_i^T \bar{C}_i + \eta P_{s,i} & -\bar{C}_i^T \\ 0 & -\bar{C}_i & \beta^2 I - I \end{bmatrix}. \quad (20)$$

By using projection lemma, we express (20) as

$$\begin{bmatrix} 0 & P_{s,i} & 0 \\ P_{s,i} & \Delta_a & -\bar{C}_i^T \\ 0 & -\bar{C}_i & \beta^2 I - I \end{bmatrix} + He \left( \begin{bmatrix} -I \\ \bar{A}_i^T \\ \bar{B}_{fi}^T \end{bmatrix} [Z_{s,i1} \ Z_{s,i2} \ 0] \right),$$

where  $\Delta_a = -\bar{C}_i^T \bar{C}_i + \eta P_i$ . Set  $Z_{s,i2} = a_1 Z_{s,i1}$ . Apply Schur complement we get

$$\begin{bmatrix} -He(Z_{s,i1}) & \nabla & Z_{s,i1}^T \bar{B}_{fi} \\ * & \nabla_{he} + \nabla'' & \nabla_1 \\ * & * & \beta^2 I - I \end{bmatrix} \leq 0. \quad (21)$$

The bilinear matrix inequality (21) is modified to LMI by substituting the values of  $\bar{A}_i, \bar{B}_{fi}, \bar{C}_i$  and  $R_{s,i} = Z_{s,i22}^T G_i$ . Also,  $P_{s,i}$  and  $Z_{s,i1}$  are symmetric matrices of appropriate dimension.

$$\begin{bmatrix} \psi_{11} & \psi_{12} & \psi_{13} & \psi_{14} & \psi_{15} \\ * & \psi_{22} & \psi_{23} & \psi_{24} & \psi_{25} \\ * & * & \psi_{33} & \psi_{34} & \psi_{35} \\ * & * & * & \psi_{44} & \psi_{45} \\ * & * & * & * & \psi_{55} \end{bmatrix} < 0, \quad (22)$$

where

$$\begin{aligned} \psi_{11} &= -Z_{s,i11} - Z_{s,i11}^T, \quad \psi_{12} = 0, \\ \psi_{13} &= P_{s,i11} - a_1 Z_{s,i11} + Z_{s,i11}^T A_i, \quad \psi_{14} = 0, \\ \psi_{15} &= 0, \quad \psi_{22} = -Z_{s,i22} - Z_{s,i22}^T, \quad \psi_{23} = 0, \\ \psi_{24} &= P_{s,i22} - a_1 Z_{s,i22} + Z_{s,i22}^T A_i - R_{s,i} C_i, \end{aligned}$$

$$\begin{aligned} \psi_{33} &= a_1 A_i^T Z_{s,i11} + a_1 Z_{s,i11}^T A_i + \eta P_{s,i11}, \\ \psi_{44} &= a_1 A_i^T Z_{s,i22} - a_1 C_i^T R_{s,i}^T + a_1 Z_{s,i22}^T A_i - a_1 R_{s,i} C_i \\ &\quad - C_i^T C_i + \eta P_{s,i22}, \\ \psi_{45} &= -C_i^T - a_1 R_{s,i}, \quad \psi_{25} = -R_{s,i}, \quad \psi_{34} = 0, \\ \psi_{35} &= 0, \quad \psi_{55} = \beta^2 I - I. \end{aligned}$$

Now the augmented form of switched system (8) is analyzed for unmatched period in which the  $j$ th subsystem and the  $i$ th observer is active.

Choose the Lyapunov function for unmatched time period as

$$V_{ij}(\mathfrak{J}(t)) = \mathfrak{J}^T(t) P_{s,ij} \mathfrak{J}(t). \quad (23)$$

Take derivative of (23) over the path of system (8), we have

$$\dot{V}_{ij}(\mathfrak{J}(t)) = \dot{\mathfrak{J}}^T(t) P_{s,ij} \mathfrak{J}(t) + \mathfrak{J}^T(t) P_{s,ij} \dot{\mathfrak{J}}(t). \quad (24)$$

Lemma 1 is modified during unmatched period to satisfy  $H_-$  performance

$$\dot{V}_{ij}(\mathfrak{J}(t)) - \rho V_{ij}(\mathfrak{J}(t)) - r^T(t)r(t) + \beta^2 f_s^T(t)f_s(t) \leq 0. \quad (25)$$

Substitute (23), (24) and  $r(t)$  from (8) into (25)

$$\begin{aligned} &\dot{\mathfrak{J}}^T(t) P_{s,ij} \mathfrak{J}(t) + \mathfrak{J}^T(t) P_{s,ij} \dot{\mathfrak{J}}(t) - \rho \mathfrak{J}^T(t) P_{s,ij} \mathfrak{J}(t) \\ &\quad + \beta^2 f_s^T(t)f_s(t) - [\bar{C}_i \mathfrak{J}(t) + f_s(t)]^T \\ &\quad \times [\bar{C}_i \mathfrak{J}(t) + f_s(t)] \leq 0. \end{aligned} \quad (26)$$

By substituting the expression  $\dot{\mathfrak{J}}(t)$  from (8) into (26) yields

$$\begin{aligned} &\mathfrak{J}^T(t) \bar{A}_{ij}^T P_{s,ij} \mathfrak{J}(t) + f_s^T(t) \bar{B}_{fij}^T P_{s,ij} \mathfrak{J}(t) \\ &\quad + \mathfrak{J}^T(t) P_{s,ij} \bar{A}_{ij} \mathfrak{J}(t) + \mathfrak{J}^T(t) P_{s,ij} \bar{B}_{fij} f_s(t) \\ &\quad - \rho \mathfrak{J}^T(t) P_{s,ij} \mathfrak{J}(t) - \mathfrak{J}^T(t) \bar{C}_{ij}^T \bar{C}_{ij} \mathfrak{J}(t) \\ &\quad - \mathfrak{J}^T(t) \bar{C}_{ij}^T f_s(t) - f_s^T(t) \bar{C}_{ij} \mathfrak{J}(t) - f_s^T(t) f_s(t) \\ &\quad + \beta^2 f_s^T(t) f_s(t) - 2\eta \|\mathfrak{J}(t)\| \leq 0. \end{aligned} \quad (27)$$

Rewrite (27) as

$$\begin{bmatrix} \mathfrak{J}^T(t) & f_s^T(t) \end{bmatrix} H_1 \begin{bmatrix} \mathfrak{J}(t) \\ f_s(t) \end{bmatrix} \leq 0. \quad (28)$$

Here,  $H_1 < 0$ , where

$$H_1 = \begin{bmatrix} \Delta_b & P_{s,ij} \bar{B}_{fij} - \bar{C}_{ij}^T \\ * & \beta^2 I - I \end{bmatrix}. \quad (29)$$

Here  $\Delta_b = \bar{A}_{ij}^T P_{s,ij} + P_{s,ij} \bar{A}_{ij} - \rho P_{s,ij} - \bar{C}_{ij}^T \bar{C}_{ij}$ . Also, (29) is written into the following form

$$\begin{bmatrix} \bar{A}_{ij}^T & I & 0 \\ \bar{B}_{fij}^T & 0 & I \end{bmatrix} \Pi_1 \begin{bmatrix} \bar{A}_{ij} & \bar{B}_{fij} \\ I & 0 \\ 0 & I \end{bmatrix} < 0, \quad (30)$$

where

$$\Pi_1 = \begin{bmatrix} 0 & P_{s,ij} & 0 \\ P_{s,ij} & -\bar{C}_{ij}^T \bar{C}_{ij} - \wp P_{s,ij} & -\bar{C}_{ij}^T \\ 0 & -\bar{C}_{ij} & \beta^2 I - I \end{bmatrix}. \quad (31)$$

Apply projection lemma to (31) gives

$$\begin{bmatrix} 0 & P_{s,ij} & 0 \\ P_{s,ij} & \Delta_c & -\bar{C}_{ij}^T \\ 0 & -\bar{C}_{ij} & \beta^2 I - I \end{bmatrix} + He \left( \begin{bmatrix} -I \\ \bar{A}_{ij}^T \\ \bar{B}_{fij}^T \end{bmatrix} [Z_{s,ij1} \quad Z_{s,ij2} \quad 0] \right),$$

where  $\Delta_c = -\bar{C}_{ij}^T \bar{C}_{ij} - \wp P_{s,ij}$ . Apply Schur complement and set  $Z_{s,ij2} = a_2 Z_{s,ij1}$ , we get

$$\begin{bmatrix} -He(Z_{s,ij1}) & \nabla_2 & Z_{s,ij1}^T \bar{B}_{fij} \\ * & \Delta_{fe} & \nabla_4 \\ * & * & \beta^2 I - I \end{bmatrix} \leq 0, \quad \Delta_{fe} = He(Z_{s,ij1}^T \bar{A}_{ij}) a_2 + \nabla_3. \quad (32)$$

Hence, the bilinear matrix inequality (32) is transformed into LMI by substituting the values of  $\bar{A}_{ij}$ ,  $\bar{B}_{fij}$ ,  $\bar{C}_{ij}$  and  $R_{s,ij} = Z_{s,ij22}^T G_i$ . Also,  $P_{s,ij}$  and  $Z_{s,ij1}$  are symmetric matrices of appropriate dimension.

$$\begin{bmatrix} \Psi_{11} & \Psi_{12} & \Psi_{13} & \Psi_{14} & \Psi_{15} \\ * & \Psi_{22} & \Psi_{23} & \Psi_{24} & \Psi_{25} \\ * & * & \Psi_{33} & \Psi_{34} & \Psi_{35} \\ * & * & * & \Psi_{44} & \Psi_{45} \\ * & * & * & * & \Psi_{55} \end{bmatrix} < 0, \quad (33)$$

where

$$\begin{aligned} \Psi_{11} &= -Z_{s,ij11} - Z_{s,ij11}^T, \quad \Psi_{12} = 0, \\ \Psi_{13} &= P_{s,ij11} - a_2 Z_{s,ij11} + Z_{s,ij11}^T A_j, \quad \Psi_{14} = 0, \\ \Psi_{15} &= 0, \quad \Psi_{22} = -Z_{s,ij22} - Z_{s,ij22}^T, \quad \Psi_{25} = -R_{ij}, \\ \Psi_{23} &= Z_{s,ij22}^T A_j - Z_{s,ij22}^T A_i + R_{s,ij} C_i - R_{s,ij} C_j, \\ \Psi_{24} &= P_{s,ij22} - a_2 Z_{s,ij22} + Z_{s,ij22}^T A_i - R_{s,ij} C_i, \\ \Psi_{33} &= a_2 A_j^T Z_{s,ij11} + a_2 Z_{s,ij11}^T A_j - C_j^T C_j + C_j^T C_i \\ &\quad + C_i^T C_j - C_i^T C_i - \wp P_{s,ij11}, \quad \Psi_{35} = -C_j^T + C_i^T, \\ \Psi_{44} &= a_2 A_i^T Z_{s,ij22} - a_2 C_i^T R_{s,ij} + a_2 Z_{s,ij22}^T A_i \\ &\quad - a_2 R_{s,ij} C_i - C_i^T C_i - \wp P_{s,ij22}, \quad \Psi_{55} = \beta^2 I - I, \\ \Psi_{45} &= -C_i^T - a_2 R_{s,ij}. \quad \square \end{aligned}$$

### 3.2. $H_\infty$ formulation

Consider the switched error dynamic systems (3) and (4). The  $H_\infty$  performance is satisfied which follows the assumption  $f_s(t) = 0$  as

$$\begin{cases} \dot{\mathfrak{J}}(t) = \bar{A}_i \mathfrak{J}(t) + \bar{B}_{di} d(t) - \vartheta_i(t), \\ r(t) = \bar{C}_i \mathfrak{J}(t) + \bar{D}_{di} d(t), \end{cases} \quad (34)$$

$$\begin{cases} \dot{\mathfrak{J}}(t) = \bar{A}_{ij} \mathfrak{J}(t) + \bar{B}_{dij} d(t) - \vartheta_{ij}(t), \\ r(t) = \bar{C}_{ij} \mathfrak{J}(t) + \bar{D}_{dij} d(t), \end{cases} \quad (35)$$

where the system matrices are

$$\begin{cases} \bar{A}_i = \begin{bmatrix} A_i & 0 \\ 0 & A_i - G_i C_i \end{bmatrix}, \quad \bar{D}_{di} = F_{di}, \\ \bar{B}_{di} = \begin{bmatrix} E_{di} \\ E_{di} - G_i F_{di} \end{bmatrix}, \quad \bar{C}_i = [0 \quad C_i], \\ \bar{A}_{ij} = \begin{bmatrix} A_j & 0 \\ A_{21} & A_i - G_i C_i \end{bmatrix}, \\ A_{21} = A_j - A_i + G_i C_i - G_i C_j, \\ \bar{B}_{dij} = \begin{bmatrix} E_{dj} \\ E_{dj} - G_i F_{dj} \end{bmatrix}, \quad \bar{D}_{dij} = F_{dj}, \\ \bar{C}_{ij} = [C_j - C_i \quad C_i]. \end{cases}$$

**Lemma 2** [30]: Given positive scalars  $0 < \eta < 1$ ,  $\gamma > 0$ ,  $\wp > 0$ ,  $\mu_1 \geq 1$  and  $\mu_2 \geq 1$ , if the Lyapunov function candidates  $V_i(\mathfrak{J}(t))$  and  $V_{ij}(\mathfrak{J}(t))$  exist so that following inequalities are satisfied

$$\begin{aligned} V_j(\mathfrak{J}(t)) &\leq \mu_1 V_{ij}(\mathfrak{J}(t)), \quad V_{ij}(\mathfrak{J}(t)) \leq \mu_2 V_i(\mathfrak{J}(t)), \\ \dot{V}_i(\mathfrak{J}(t)) &\leq -\eta V_i(\mathfrak{J}(t)) - \Upsilon'_1, \\ \dot{V}_{ij}(\mathfrak{J}(t)) &\leq \wp V_{ij}(\mathfrak{J}(t)) - \Upsilon'_1, \end{aligned}$$

where  $\Upsilon'_1 = r^T(t)r(t) - \gamma^2 d^T(t)d(t)$ , then system satisfies global asymptotic stability and obtain  $H_\infty$  performance along with ADT.

**Theorem 2:** Given positive constants  $0 < \eta < 1$ ,  $\wp > 0$ ,  $\gamma > 0$ ,  $b_1 > 1$  and  $b_2 > 1$  then switched system (1) and fault detection sliding mode observer (2) achieve global asymptotic stability and satisfies  $H_\infty$  performance (6) and switching signal besides ADT (9), provided that there exist positive definite symmetric matrices  $P_{r,i} > 0$ ,  $P_{r,ij} > 0$ ,  $Z_{r,i1} > 0$ ,  $Z_{r,ij1} > 0$ ,  $Z_{r,i2} > 0$  and  $Z_{r,ij2} > 0$ , such that following inequalities hold

$$\begin{bmatrix} -He(Z_{r,i1}) & \Delta'_i & Z_{r,i1}^T \bar{B}_{di} \\ * & \Delta'_{hi} + \Delta'_e & \Delta'_1 \\ * & * & \Delta'_2 \end{bmatrix} \leq 0, \quad (36)$$

$$\begin{bmatrix} -He(Z_{r,ij1}) & \Delta'_j & \Delta'_4 \\ * & \Delta'_{hj} + \Delta'_3 & \Delta'_5 \\ * & * & \Delta'_6 \end{bmatrix} \leq 0, \quad (37)$$

where  $\Delta'_i = P_{r,i} - b_1 Z_{r,i1} + Z_{r,i1}^T \bar{A}_i$ ,  $\Delta'_{hi} = He(Z_{r,i1}^T \bar{A}_i) b_1$ ,  $\Delta'_e = \bar{C}_i^T \bar{C}_i + \eta P_{r,i}$ ,  $\Delta'_1 = \bar{C}_i^T \bar{D}_{di} + b_1 Z_{r,i1}^T \bar{B}_{di}$ ,  $\Delta'_2 = -\gamma^2 I + \bar{D}_{di}^T \bar{D}_{di}$ ,  $\Delta'_j = P_{r,ij} - b_2 Z_{r,ij1} + Z_{r,ij1}^T \bar{A}_{ij}$ ,  $\Delta'_{hj} = He(Z_{r,ij1}^T \bar{A}_{ij}) b_2$ ,  $\Delta'_3 = \bar{C}_{ij}^T \bar{C}_{ij} - \wp P_{s,ij}$ ,  $\Delta'_4 = Z_{r,ij1}^T \bar{B}_{dij}$ ,  $\Delta'_5 = \bar{C}_{ij}^T \bar{D}_{dij} + b_2 Z_{r,ij1}^T \bar{B}_{dij}$ , and  $\Delta'_6 = -\gamma^2 I + \bar{D}_{dij}^T \bar{D}_{dij}$ .

**Remark 2:** Asynchronous switched systems utilize the  $H_\infty$  approach to devise a control strategy that mitigates the effect of disturbances on the residual signal during

matched and unmatched periods. Furthermore, the  $H_\infty$  design criteria ensure that the residual signal is attenuated in the presence of disturbances. Consequently, the observer can maintain the stability of the system, even when confronted with disturbances in the asynchronous switching phenomenon, and ensure that the residual signal is effectively attenuated.

**Proof:** To derive the results of  $H_\infty$  performance from Theorem 2, we employ the Lyapunov function  $V_i(\tilde{\mathfrak{J}}(t)) = \tilde{\mathfrak{J}}^T(t)P_{r,i}\tilde{\mathfrak{J}}(t)$  and  $V_{ij}(\tilde{\mathfrak{J}}(t)) = \tilde{\mathfrak{J}}^T(t)P_{r,ij}\tilde{\mathfrak{J}}(t)$  for both matched and unmatched periods, respectively. Thus applying Lemma 2 and solving the inequalities respectively while using the same procedure as done earlier in  $H_-$  formulation from Theorem 1. The following LMIs are obtained by solving the inequalities (36) and (37) respectively for matched and unmatched periods of asynchronous switched systems.

$$\begin{bmatrix} \Xi_{11} & \Xi_{12} & \Xi_{13} & \Xi_{14} & \Xi_{15} \\ * & \Xi_{22} & \Xi_{23} & \Xi_{24} & \Xi_{25} \\ * & * & \Xi_{33} & \Xi_{34} & \Xi_{35} \\ * & * & * & \Xi_{44} & \Xi_{45} \\ * & * & * & * & \Xi_{55} \end{bmatrix} < 0, \quad (38)$$

$$\begin{bmatrix} Y_{11} & Y_{12} & Y_{13} & Y_{14} & Y_{15} \\ * & Y_{22} & Y_{23} & Y_{24} & Y_{25} \\ * & * & Y_{33} & Y_{34} & Y_{35} \\ * & * & * & Y_{44} & Y_{45} \\ * & * & * & * & Y_{55} \end{bmatrix} < 0, \quad (39)$$

where

$$\begin{aligned} \Xi_{11} &= -Z_{r,i11} - Z_{r,i11}^T, \quad \Xi_{13} = P_{r,i11} - b_1 Z_{r,i11} \\ &\quad + Z_{r,i11}^T A_i, \\ \Xi_{15} &= Z_{r,i11}^T E_{di}, \quad \Xi_{22} = -Z_{r,i22} - Z_{r,i22}^T, \\ \Xi_{24} &= P_{r,i22} - b_1 Z_{r,i22} + Z_{r,i22}^T A_i - R_{r,i} C_i, \\ \Xi_{33} &= b_1 A_i^T Z_{r,i11} + b_1 Z_{r,i11}^T A_i + \eta P_{r,i11}, \\ \Xi_{44} &= b_1 A_i^T Z_{r,i22} - b_1 C_i^T R_{r,i}^T + b_1 Z_{r,i22}^T A_i - b_1 R_{r,i} C_i \\ &\quad + C_i^T C_i + \eta P_{r,i22}, \\ \Xi_{35} &= b_1 Z_{r,i11} E_{di}, \\ \Xi_{45} &= C_i^T F_{di} + b_1 Z_{r,i22}^T E_{di} - b_1 R_{r,i} F_{di}, \\ \Xi_{25} &= Z_{r,i22} E_{di} - R_{r,i} F_{di}, \quad \Xi_{55} = -\gamma^2 I + F_{di} F_{di}, \\ Y_{11} &= -Z_{r,ij11} - Z_{r,ij11}^T, \quad Y_{12} = 0, \\ Y_{13} &= P_{r,ij11} - b_2 Z_{r,ij11} + Z_{r,ij11}^T A_j, \quad Y_{14} = 0, \\ Y_{15} &= Z_{r,i11}^T E_{dj}, \quad Y_{22} = -Z_{r,ij22} - Z_{r,ij22}^T, \\ Y_{23} &= Z_{r,ij22}^T A_j - Z_{r,ij22}^T A_i + R_{r,ij} C_i - R_{r,ij} C_j, \\ Y_{24} &= P_{r,ij22} - b_2 Z_{r,ij22} + Z_{r,ij22}^T A_i - R_{r,ij} C_i, \\ Y_{25} &= Z_{r,ij22}^T E_{dj} - R_{r,ij} F_{dj}, \\ Y_{33} &= b_2 A_j^T Z_{r,ij11} + b_2 Z_{r,ij11}^T A_j + C_j^T C_j - C_j^T C_i \\ &\quad - C_i^T C_j + C_i^T C_i - \wp P_{r,ij11}, \end{aligned}$$

$$\begin{aligned} Y_{35} &= C_j^T F_{dj} - C_i^T F_{dj} + b_2 Z_{r,ij11}^T E_{dj}, \\ Y_{44} &= b_2 A_i^T Z_{r,ij22} - b_2 C_i^T R_{r,ij}^T + b_2 Z_{r,ij22}^T A_i \\ &\quad - b_2 R_{r,ij} C_i + C_i^T C_i - \wp P_{r,ij22}, \\ Y_{45} &= C_i^T F_{dj} + b_2 Z_{r,ij22}^T E_{dj} - b_2 R_{r,ij} F_{dj}, \\ Y_{55} &= -\gamma^2 I + F_{dj} F_{dj}. \end{aligned} \quad \square$$

### 3.3. Mixed $H_-/H_\infty$ formulation

In this section, the mixed  $H_-/H_\infty$  performance is introduced to provide an efficient combination of fault sensitivity and disturbance robustness. The mixed  $H_-/H_\infty$  performance solution refers to a control methodology designed to tackle the problem of asynchronous switching in systems subject to faults and disturbances. Asynchronous switching occurs when the switching times of the observer and subsystem are not synchronized, which can lead to the instability of the system. The mixed  $H_-/H_\infty$  performance strategy blends two distinct control objectives:  $H_-$  control, which seeks to maximize the sensitivity of fault to residual, and  $H_\infty$  control, which aims to minimize the impact of disturbances on the residual signal. The overall goal of the mixed  $H_-/H_\infty$  performance approach is to address the challenge of asynchronous switching in control systems by providing robust fault detection that can maintain stability and performance even in the presence of faults and disturbances in the system.

**Theorem 3:** The systems (3) and (4) are asymptotically stable and achieves  $H_-/H_\infty$  performance indices (5) and (6), if there exist symmetric matrices  $P_{s,i} = P_{r,i} = P_i$ ,  $P_{s,ij} = P_{r,ij} = P_{ij}$ ,  $Z_{s,i1} = Z_{r,i1} = Z_{i1}$ ,  $Z_{s,ij1} = Z_{r,ij1} = Z_{ij1}$  as derived from Theorems 1 and 2 respectively, and positive scalars  $0 < \eta < 1$ ,  $\wp > 0$ ,  $\beta > 0$ ,  $\gamma > 0$ , such that the following inequalities hold.

$$\begin{bmatrix} -He(Z_{i1}) & \nabla & Z_{i1}^T \bar{B}_{fi} \\ * & \nabla_{he} + \nabla'' & \nabla_1 \\ * & * & \beta^2 I - I \end{bmatrix} \leq 0, \quad (40)$$

$$\begin{bmatrix} -He(Z_{ij1}) & \nabla_2 & Z_{ij1}^T \bar{B}_{fij} \\ * & \nabla'_{he} + \nabla'_3 & \nabla_4 \\ * & * & \beta^2 I - I \end{bmatrix} \leq 0, \quad (41)$$

$$\begin{bmatrix} -He(Z_{i1}) & \Delta'_i & Z_{i1}^T \bar{B}_{di} \\ * & \Delta'_{hi} + \Delta'_e & \Delta'_1 \\ * & * & \Delta'_2 \end{bmatrix} \leq 0, \quad (42)$$

$$\begin{bmatrix} -He(Z_{ij1}) & \Delta'_j & \Delta'_4 \\ * & \Delta'_{hj} + \Delta'_3 & \Delta'_5 \\ * & * & \Delta'_6 \end{bmatrix} \leq 0, \quad (43)$$

where  $\nabla = P_i - a_1 Z_{i1} + Z_{i1}^T \bar{A}_i$ ,  $\nabla''_{he} = He(Z_{i1}^T \bar{A}_i) a_1$ ,  $\nabla'' = -\bar{C}_i^T \bar{C}_i + \alpha P_i$ ,  $\nabla_1 = -\bar{C}_i^T + a_1 Z_{i1}^T \bar{B}_{fi}$ ,  $\nabla_2 = P_{ij} - a_2 Z_{ij1} + Z_{ij1}^T \bar{A}_{ij}$ ,  $\nabla_{he} = He(Z_{ij1}^T \bar{A}_{ij}) a_2$ ,  $\nabla_3 = -\bar{C}_{ij}^T \bar{C}_{ij} - \wp P_{ij}$  and  $\nabla_4 = -\bar{C}_{ij}^T + a_2 Z_{ij1}^T \bar{B}_{fij}$ ,  $\Delta'_i = P_i - b_1 Z_{i1} + Z_{i1}^T \bar{A}_i$ ,  $\Delta'_{hi} = He(Z_{i1}^T \bar{A}_i) b_1$ ,  $\Delta'_e = \bar{C}_i^T \bar{C}_i + \eta P_i$ ,  $\Delta'_1 = \bar{C}_i^T \bar{D}_{di} + b_1 Z_{i1}^T \bar{B}_{di}$ ,  $\Delta'_2 = -\gamma^2 I + \bar{D}_{di}^T \bar{D}_{di}$ ,  $\Delta'_j = P_{ij} - b_2 Z_{ij1} + Z_{ij1}^T \bar{A}_{ij} \Delta'_{hj} =$



$He(Z_{ij1}^T \bar{A}_{ij}) b_2, \Delta_3 = \bar{C}_{ij}^T \bar{C}_{ij} - \wp P_{ij}, \Delta_4 = Z_{r,ij1}^T \bar{B}_{dij}, \Delta_5 = \bar{C}_{ij}^T \bar{D}_{dij} + b_2 Z_{ij1}^T \bar{B}_{dij},$  and  $\Delta_6 = -\gamma^2 I + \bar{D}_{dij}^T \bar{D}_{dij}.$

Moreover the observer parameters for mixed  $H_-/H_\infty$  are obtained as

**Observer parameters for matched period:**

$$G_i = (Z_{i22}^{-1})^T R_i, \quad \vartheta_i(t) = \rho P_i^{-1} \frac{e(t)}{\|e(t)\|}.$$

**Observer parameters for unmatched period:**

$$G_i = (Z_{ij22}^{-1})^T R_{ij}, \quad \vartheta_{ij}(t) = \rho P_{ij}^{-1} \frac{e(t)}{\|e(t)\|}.$$

**Proof:** Theorem 3 is straightforwardly deduced from Theorems 1 and 2. As a result, its proof is omitted here.  $\square$

**Remark 3:** The mixed  $H_-/H_\infty$  performance control strategy is designed to address the challenges of maintaining stability in a switched system under disturbances and faults while achieving good sensitivity performance ( $H_-$ ) and disturbance rejection performance ( $H_\infty$ ). This is achieved by formulating the design problem with mixed  $H_-/H_\infty$  performance and selecting a Lyapunov function along with average dwell time during matched and unmatched periods to ensure stability. The observer parameters and desired matrix variables are obtained using linear matrix inequalities (LMIs).

### 3.4. Algorithm

Let the switched system model and SMO based FD system synthesis be given in (1) and (2).

**Inputs for Step 1** ( $A_i, C_i$ ):

**Step 1:** First, check the observability of all the modes (subsystems), such that  $(A_i, C_i)$  is observable.

**Output for Step 1** (Observability check):

**Step 2:** Established the augmented systems for both matched and unmatched periods of asynchronous switching phenomena in the form of (7), (8), (38) and (39). Meanwhile choose a Lyapunov function along with ADT to achieve stability of switched system. Also compute the coefficients of augmented system matrices including  $\bar{A}_i, \bar{A}_{ij}, \bar{C}_i, \bar{C}_{ij}, \bar{B}_{fi}, \bar{B}_{fij}, \bar{D}_{di}$  and  $\bar{D}_{dij}.$

**Inputs for Step 3** (Fault  $f(t), \beta$ ):

**Step 3:** For fault sensitivity to residual signal, construct an FD system that meets the  $H_-$  performance (5) index and solves LMIs using Theorem 1.

**Output for Step 3** (Sensitivity to the fault):

**Inputs for Step 4** (Disturbance  $d(t), \gamma$ ):

**Step 4:** Design the FD system so that  $H_\infty$  performance index (6) holds and Theorem 2 provides the LMI solution for residual signal robust to disturbance only.

**Output for Step 4** (Robustness to disturbance):

**Step 5:** A mixed  $H_-/H_\infty$  performance indices (5) and (6) must be met for the residual signal to be both fault sensitive and robust against process disturbance. We also

specify the parameters for the mixed  $H_-/H_\infty$  by setting  $P_{s,i} = P_{r,i} = P_i, P_{s,ij} = P_{r,ij} = P_{ij}, Z_{s,i1} = Z_{r,i1} = Z_{i1}, Z_{s,ij1} = Z_{r,ij1} = Z_{ij1}, R_{s,i} = R_{r,i} = R_i, R_{s,ij} = R_{r,ij} = R_{ij}.$

### 3.5. Residual evaluation

In addition to residual signal generation, the most significant step is the evaluation of residual signal. Sometimes the problem of false alarms are observed in the system, because residual signal is nonzero even in the absence of faults. Therefore it is necessary to compute residual evaluation step.

$$J_e(t) = \sqrt{\frac{1}{\aleph} \int_0^{\aleph} r_y^T(t) r_y(t) dt}. \quad (44)$$

The difficulty of false FD is overcome by calculating the threshold along with evaluated residual. Thus threshold is measured for zero fault case in the presence of disturbances.

$$J_{th} = \sup_{f(t)=0} J_e(t). \quad (45)$$

For effective FD, the evaluated residual is compared to that of threshold. Thus any exceed of this evaluated residual from the threshold signal results in FD occurs, or else no fault is detected.

## 4. SIMULATION STUDY

### 4.1. Case study of buck-boost converter

A buck-boost converter circuit consists of buck and boost converter elements, respectively, as in Fig. 3. This circuit type delivers a voltage above or below the regulated output voltage. Considering the sensor fault occurs in the inductor and capacitor incorporated into two subsystems; where  $i_L$  is inductor current and  $v_c$  is capacitor voltage. The state space model of the buck-boost converter is described as

$$A_{\sigma(t)} = \begin{bmatrix} 0 & \frac{1-s(t)}{L} \\ -\frac{1-s(t)}{C} & -\frac{1}{R_0 C} \end{bmatrix},$$

$$B_{\sigma(t)} = \begin{bmatrix} \frac{s(t)v_s}{L} \\ 0 \end{bmatrix}, \quad x(t) = \begin{bmatrix} v_c(t) \\ i_L(t) \end{bmatrix}.$$

The switching signal  $\sigma(t)$  has two operating modes as  $\sigma(t) = [1, 2]$  as shown in Table 1. Subsystems and ob-

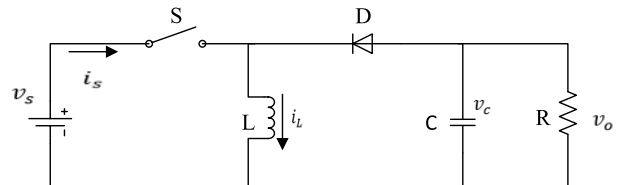


Fig. 3. Buck-boost converter circuit.

**Table 1.** Open/close positions of switch system.

|    | $\sigma(t)$ | 1 | 2 |
|----|-------------|---|---|
| 1) | $S_1$       | 1 | 0 |
| 2) | $S_2$       | 0 | 1 |

**Table 2.** Parameters of buck-boost converter.

|    | Symbol | Name           | Value                   |
|----|--------|----------------|-------------------------|
| 1) | $L$    | Inductance     | $4.5 \times 10^{-3}$ H  |
| 2) | $C$    | Capacitance    | $1.04 \times 10^{-5}$ F |
| 3) | $R_0$  | Resistance     | 12 $\Omega$             |
| 4) | $v_s$  | Input voltage  | 40 V                    |
| 5) | $v_o$  | output voltage | -24 V                   |

servers function asynchronously during their respective time periods. When subsystem 1 and observer 1 act synchronously or in matched time, mode 1 is triggered. The system functions asynchronously or with a mismatch time condition when the switching system shifts to subsystem 2 while the observer remains in its prior mode (observer 1). The dynamic of the system matrices is obtained by taking  $s(t) = 1$  and  $s(t) = 0$  to activate mode 1 and mode 2, respectively as in [46]. For the buck-boost converter simulation, the circuit parameters in Fig. 3 are set to the following values in Table 2.

$$A_1 = \begin{bmatrix} 0 & 0 \\ 0 & -8012.82 \end{bmatrix}, B_1 = \begin{bmatrix} 8888.88 \\ 0 \end{bmatrix},$$

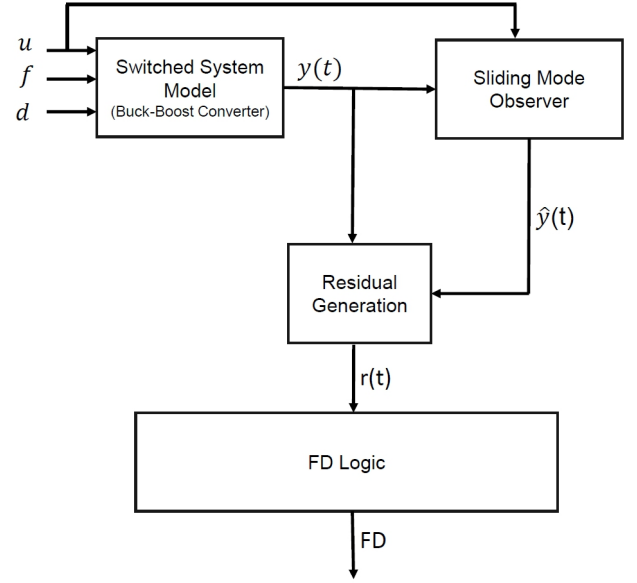
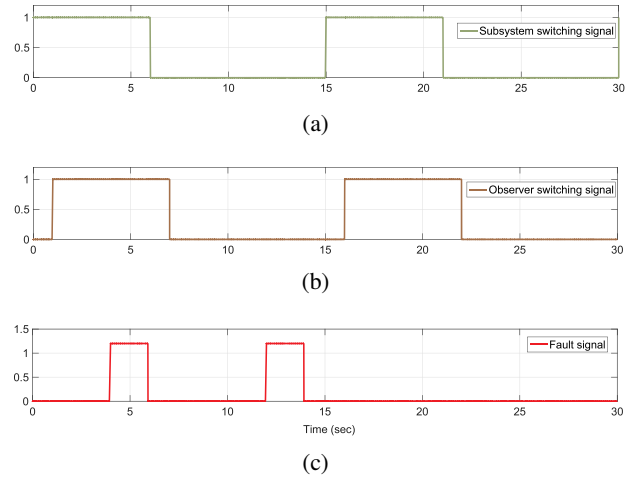
$$C_1 = \begin{bmatrix} 1 & 0 \\ 0 & -1 \end{bmatrix}, E_{d1} = \begin{bmatrix} 0.1 & -0.3 \\ 0.4 & -0.1 \end{bmatrix},$$

$$A_2 = \begin{bmatrix} 0 & 222.22 \\ -96153.84 & -8012.82 \end{bmatrix}, F_{d1} = 0.2,$$

$$B_2 = \begin{bmatrix} 0 \\ 0 \end{bmatrix}, C_2 = \begin{bmatrix} 1 & 0 \\ 0 & -1 \end{bmatrix},$$

$$E_{d2} = \begin{bmatrix} -0.2 & 0.3 \\ 0.1 & -0.5 \end{bmatrix}, F_{d2} = 0.5.$$

The block diagram presented in Fig. 4 illustrates a robust FD scheme for switched system model of the buck-boost converter operating in the presence of faults and disturbances. Subsequently, SMO is designed for each subsystem of the switched system. The SMOs generate residual signals by computing the difference between the actual and estimated outputs. Additionally, FD logic is incorporated in the scheme, which includes residual evaluation and threshold computation, to enable effective fault detection. For the effectiveness of the proposed scheme, MATLAB/Simulink is used. Set the simulation time to 30 seconds. The asynchronous switching behavior of the subsystem and observer is shown in Fig. 5. During the matched period, the subsystem and observer switch between 1-6, 7-15, 16-21, and 22-30 seconds. The time intervals throughout the unmatched period of subsystem and ob-

**Fig. 4.** Block diagram of robust fault detection scheme.**Fig. 5.** (a) Subsystem switching signal. (b) Observer switching signal. (c) Fault signal.

server switching, on the other hand, are 0-1, 6-7, and 15-16 seconds in Figs. 5(a) and 5(b), respectively. Fig. 5(c) shows the fault signal of a pulse generator with magnitude  $f(t) = 1.2$ . Faults occur in subsystems of the switched system during mode 1 and mode 2, respectively.

Furthermore, setting constant parameters  $\eta = 0.1$ ,  $\beta = 1.5$ ,  $\mu_1 = \mu_2 = 1.2$ ,  $a_i = 1.5$ ,  $b_i = 1.7$ , fault sensitivity level  $\beta = 0.256$  and disturbance attenuation level  $\gamma = 0.126 \forall i \in [1, 2]$  lead to a feasible solution. Thus by applying switching signal  $\sigma(t)$ , ADT is adjusted to 1.823. This way, the switching interval exceeds the value 1.823 between two subsystems. The simulation study also includes a  $L_2$ -norm bounded disturbance signal with  $-1 \leq d \leq 1$ . Thus, by solving (40)-(43) from Theorem 3 respectively,

the simulation is used to determine the numerical values of observer parameters  $G_i$  and symmetric matrices  $P_i$ ,  $P_{ij}$ ,  $Z_{i22}$  and  $Z_{ij22}$ .

$$P_1 = \begin{bmatrix} 2.10 & -0.95 \\ -0.95 & 2.16 \end{bmatrix}, P_2 = \begin{bmatrix} 2.73 & -0.98 \\ -0.98 & 2.16 \end{bmatrix}, \quad (46)$$

$$P_{12} = \begin{bmatrix} 1.30 & -0.46 \\ -0.46 & 1.30 \end{bmatrix}, P_{21} = \begin{bmatrix} 1.55 & -0.4 \\ -0.4 & 1.34 \end{bmatrix}, \quad (47)$$

$$Z_1 = \begin{bmatrix} 0.99 & -0.44 \\ -0.44 & 1.20 \end{bmatrix}, Z_2 = \begin{bmatrix} 1.18 & -0.49 \\ -0.49 & 1.19 \end{bmatrix}, \quad (48)$$

$$Z_{12} = \begin{bmatrix} 0.52 & -0.28 \\ -0.28 & 0.85 \end{bmatrix}, Z_{21} = \begin{bmatrix} 0.59 & -0.2 \\ -0.2 & 0.76 \end{bmatrix}, \quad (49)$$

$$G_1 = \begin{bmatrix} 0.151 & 0.021 \\ 0.138 & -0.133 \end{bmatrix}, G_2 = \begin{bmatrix} -0.29 & 0.27 \\ 0.08 & 0.11 \end{bmatrix}. \quad (50)$$

The eigenvalues of  $A_i - G_i C_i$  from (3) and (4) are stable over the matched and unmatched periods of asynchronous switching, where 'i' is the mode of switched asynchronous systems. While investigating eigen values during matched and unmatched periods, the following possible cases are investigated.

**Case 1:** Eigen values of  $A_i - G_i C_i$  during matched period.

- 1)  $A_1 - G_1 C_1$  has stable eigen values if the subsystem 1 and observer 1 are operating in mode 1.
- 2)  $A_2 - G_2 C_2$  has stable eigenvalues if subsystem 2 and observer 2 are operating in mode 2.

**Case 2:** Eigen values of  $A_i - G_i C_i$  during unmatched period.

- 1)  $A_2 - G_1 C_2$  has stable eigen values, if the subsystem 2 and observer 1 are in operation.
- 2)  $A_1 - G_2 C_1$  has stable eigenvalues, if subsystem 1 and observer 2 are in operation.

The response of the residual signal with fault and disturbance effect for both subsystems is examined. Fig. 6 shows the impact of residual signal in the presence of a fault and without the use of a disturbance signal. Fig. 7 on the other hand, depicts the effect of disturbance on residual solely in the absence of any fault as input. For robust FD, we analyze the residual signal together with the threshold calculation with the help of (44) and (45). Hence, the residual signal is as sensitive to fault as possible while also being robust to disturbance. Then a fault signal of a pulse generator occurs in mode 1 at  $t = 4$  sec. Fig. 8 shows the generated residual signal for subsystem 1 with simultaneous fault and disturbance, and its evaluation with threshold  $J_{he1} = 0.16$ . Fig. 9 shows the residual signal and its evaluation with a magnitude of threshold

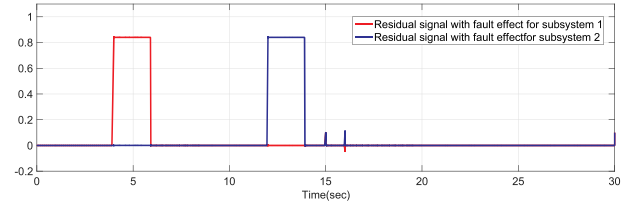


Fig. 6. Effect of residual signals with fault signal only.

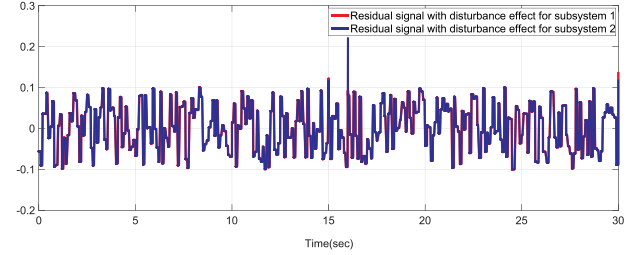
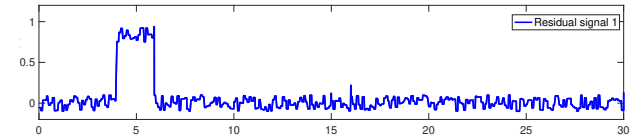
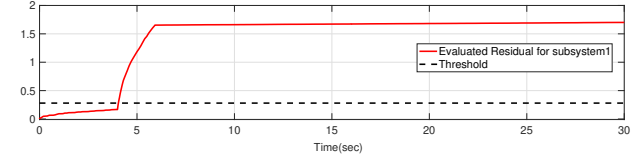


Fig. 7. Effect of residual signals with disturbance signal only.

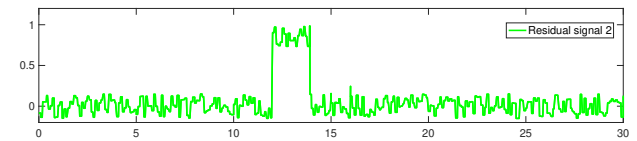


(a)

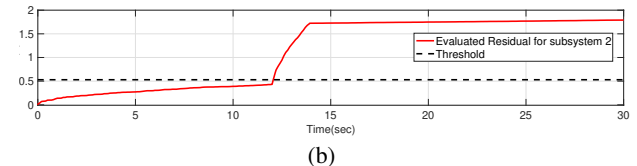


(b)

Fig. 8. (a) Residual signal for subsystem 1. (b) Evaluated residual for subsystem 1 with threshold.



(a)



(b)

Fig. 9. (a) Residual signal for subsystem 2. (b) Evaluated residual for subsystem 2 with threshold.

$J_{he2} = 0.33$  when fault and disturbance only affect subsystem 2 at time  $t = 12$  sec in mode 2. Finally, take into account the multi-type fault case shown in Fig. 10, which provides the residual signal and evaluation of residual in both subsystems at  $t = 4$  sec and  $t = 12$  sec, respectively with  $J_{he12} = 0.301$  threshold.

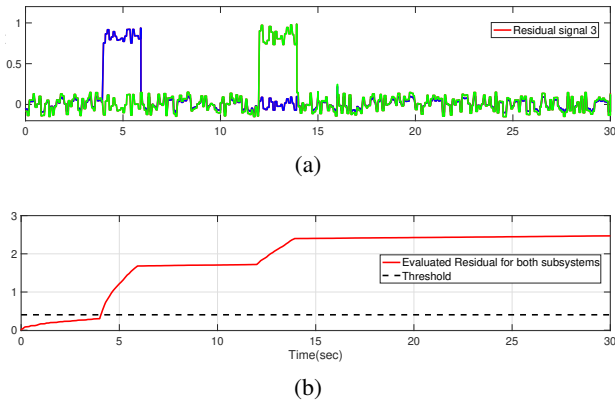


Fig. 10. (a) Residual signal for both subsystems. (b) Evaluated residual for both subsystems 1 and 2 with threshold.

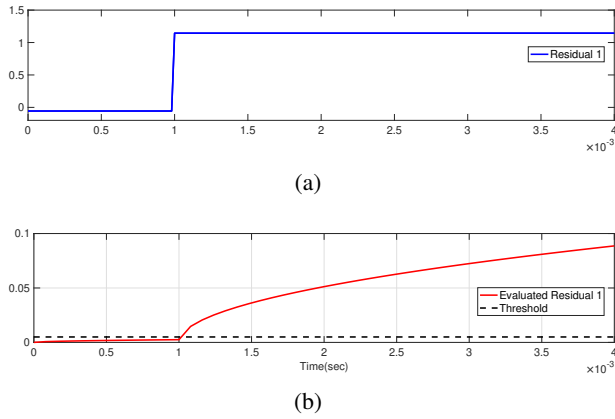


Fig. 11. (a) Residual signal under transient condition for subsystem 1. (b) Evaluated residual with threshold under transient condition for subsystem 1.

On the other hand, the simulation time is set to 0.004 seconds to examine FD under transient conditions. Transient conditions in buck-boost converter circuits are examined when a fault occurs in the converter circuit's capacitor and inductor while switching from one mode to the other. Consider the FD when SMO 1 and subsystem 1 are operational in mode 1. The residual signal and evaluation of the residual at time  $t = 0.001$  sec are shown in Fig. 11, along with the threshold  $J_{th1} = 0.003$ .

Next, the results of FD in mode 2 are examined. Here, switching happens while SMO 2 and subsystem 1 is active. The residual and its evaluation at  $t = 0.002$  sec with threshold  $J_{th1} = 0.006$  are shown in Fig. 12. Finally, consider the simultaneous FD when using both switched system modes. Fig. 13 shows the simulation results for the residuals and their evaluation signal with a threshold of  $J_{th2} = 0.0046$ .

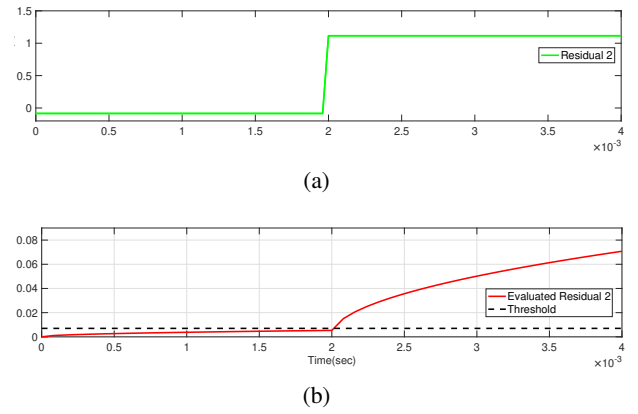


Fig. 12. (a) Residual signal under transient condition for subsystem 2. (b) Evaluated residual with threshold under transient condition for subsystem 2.

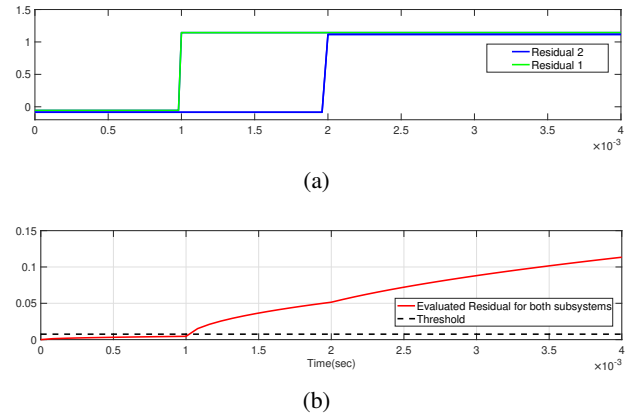


Fig. 13. (a) Residual signal under transient condition for both subsystems. (b) Evaluated residual with threshold under transient condition for both subsystems.

## 5. CONCLUSION

This research investigates fault detection for continuous-time asynchronous switched systems. The aim of fault detection sliding mode observer is to achieve fault sensitivity and robustness against disturbance through mixed  $H_2/H_\infty$  optimization technique. A piece-wise Lyapunov function is employed to solve the asynchronous switching problems during matched and unmatched periods while considering average dwell time constraints. Linear matrix inequalities are obtained to determine sufficient conditions and give feasible solutions to the proposed method. As illustrated in the simulation example, the developed mechanism is not only able to detect faults but also to determine the sensitivity and robustness of the fault. Further research is needed to enhance the safety, reliability, and performance of complex engineering sys-

tems in the context of model uncertainty. Accordingly, our future research efforts will focus on developing improved techniques for fault isolation and estimation, aiming to accurately determine the magnitude or severity of faults. This will enable the development of more effective fault tolerant control strategies tailored to the fault's specific characteristics, based on its estimated size or severity. On the other hand, time delays are an intrinsic component of many practical systems. Time delays can lead to poor performance, oscillation, or instability. Thus, sliding mode observer-based fault diagnosis in asynchronous switching time delay systems is a challenging problem that requires additional research. More recently, big data and machine learning techniques are attractive choices for data-driven and model-based fault diagnosis in asynchronous switched systems.

### CONFLICT OF INTEREST

The authors declare that there is no potential conflict of interest possibly influencing the interpretation of data in the paper. Also, there is no competing financial interest or personal relationship that could have appeared to influence the work reported in this paper.

### REFERENCES

- [1] S. X. Ding, *Model-based Fault Diagnosis Techniques*, vol. Second, Springer-Verlag London, pp. 13-116, 2013.
- [2] Z. Gao, C. Cecati, and S. X. Ding, "A survey of fault diagnosis and fault-tolerant techniques Part II: Fault diagnosis with knowledge-based and hybrid/active approaches," *IEEE Transactions on Industrial Electronics*, vol. 62, pp. 3768-3774, 2015.
- [3] R. Busch and I. K. Peddle, "Active fault detection for open loop stable LTI SISO systems," *International Journal of Control, Automation, and Systems*, vol. 12, pp. 324-332, 2014.
- [4] S. X. Ding, *Advanced Methods for Fault Diagnosis and Fault-tolerant Control*, vol. third, Springer-Verlag Germany, Part of Springer Nature, 2021.
- [5] Y. Jiang, S. Yin, and O. Kaynak, "Optimized design of parity relation based residual generator for fault detection: Data-driven approaches," *IEEE Transaction on Industrial Informatics*, vol. 17, pp. 1449-1458, 2020.
- [6] J. C. L. Chan, W. S. Chua, T. H. Lee, and C. P. Tan, "Descriptor observers for robust fault reconstruction in a class of nonlinear descriptor systems," *International Journal of Control, Automation, and Systems*, vol. 21, pp. 1-14, 2022.
- [7] M. Kordestani, M. Saif, M. E. Orchard, R. Razavi-Far, and K. Khorasani, "Failure prognosis and applications - A survey of recent literature," *IEEE Transaction on Reliability*, vol. 70, pp. 728-748, 2021.
- [8] H. Luo, S. Yin, T. Liu, and A. Q. Khan, "A data-driven realization of the control-performance-oriented process monitoring system," *IEEE Transaction on Industrial Electronics*, vol. 67, pp. 521-530, 2019.
- [9] W. Li, H. Li, S. Gu, and T. Chen, "Process fault diagnosis with model-and knowledge-based approaches: Advances and opportunities," *Control Engineering Practice*, 2020.
- [10] Y. Jiang, S. Wu, and H. Yang, "Secure data transmission and trustworthiness judgement approaches against cyber-physical attacks in an integrated data-driven framework," *IEEE Transactions on Systems, Man, and Cybernetics*, vol. 52, pp. 7799-7809, 2022.
- [11] D. Zhai, A. Lu, J. Dong, and Q. Zhang, "Event triggered  $H_-/H_\infty$  fault detection and isolation for T-S fuzzy systems with local nonlinear models," *Signal Processing*, vol. 138, pp. 244-255, 2017.
- [12] H. Sang, H. Nie, and J. Zhao, "Dwell-time-dependent asynchronous  $H_\infty$  filtering for discrete-time switched systems with missing measurements," *Signal Processing*, vol. 151, pp. 56-65, 2018.
- [13] Z. Wang, P. Shi, and C. Lim, " $H_-/H_\infty$  fault detection observer in finite frequency domain for linear parameter-varying descriptor systems," *Automatica*, vol. 86, pp. 38-45, 2017.
- [14] J. Xiong, X. H. Chang, and X. Yi, "Design of robust non-fragile fault detection filter for uncertain dynamic systems with quantization," *Applied Mathematics and Computation*, vol. 338, pp. 774-788, 2018.
- [15] X. Xiao, L. Zhou, and G. Lu, "Event-triggered  $H_\infty$  filtering of continuous-time switched linear systems," *Signal Processing*, vol. 141, pp. 343-349, 2017.
- [16] D. Liberzon, *Switching in Systems and Control*, Springer Science & Business Media, 2012.
- [17] J. Harikumar, G. Buticchi, G. Migliazzi, V. Madonna, P. Giangrande, A. Costabeber, P. Wheeler, and Mochael Galea, "Failure modes and reliability oriented system design for aerospace power electronic converters," *IEEE Open Journal of the Industrial Electronic Society*, vol. 2, pp. 53-64, 2020.
- [18] H. Zhu, "Output regulation with prescribed performance control of switched strict-feedback systems," *International Journal of Control, Automation, and Systems*, vol. 21, pp. 1-8, 2023.
- [19] R. Wang, L. Hou, G. Zong, S. Fei, and D. Yang, "Stability and stabilization of continuous-time switched systems: A multiple discontinuous convex Lyapunov function approach," *International Journal of Robust and Nonlinear Control*, vol. 29, pp. 1499-1514, 2018.
- [20] W. Xiang, "Stabilization for continuous-time switched linear systems: A mixed switching scheme," *Nonlinear Analysis: Hybrid Systems*, vol. 36, pp. 1-16, 2020.
- [21] S. Zhang, J. Zhang, X. Jia, and P. Lin, "Event-triggered asynchronous filter of switched nonlinear positive systems," *International Journal of Control, Automation, and Systems*, vol. 21, pp. 536-552, 2023.

- [22] X. Lu, G. Jing, H. Sun, X. Lyu, A. Wen, Y. Guo, and Q. Zheng, "Dynamic event-triggered quantitative feedback control for switched affine systems," *International Journal of Control, Automation, and Systems*, vol. 21, pp. 1861-1870, 2022.
- [23] J. Li, F. Jia, and X. He, "On fault detection of discrete-time switched systems via designing time-varying residual generators," *Journal of the Franklin Institute*, vol. 358, pp. 1122-1135, 2021.
- [24] Q. Su, Z. Fan, and J. Li, "Observer-based fault detection for switched systems with all unstable subsystems," *Journal of Control and Decision*, vol. 8, no. 2, pp. 116-123, 2019.
- [25] Q. Su, C. Li, X. Guo, X. Zhang, and J. Li, "Robust fault diagnosis for DC-DC Boost converters via switched systems," *Control Engineering Practice*, vol. 112, 2021.
- [26] G. X. Zhong and G. H. Yang, "Simultaneous fault detection and control for discrete-time switched systems," *Circuits, Systems, and Signal Processing*, vol. 34, pp. 3811-3831, 2015.
- [27] Y. Zhu and W. X. Zheng, "An integrated design approach for fault-tolerant control of switched LPV systems with actuator faults," *IEEE Transactions on Systems, Man, and Cybernetics: Systems*, vol. 53, 2023.
- [28] T. Sun, D. Zhou, Y. Zhu, and M. V. Basin, "Stability,  $l_2$ -gain analysis, and parity space-based fault detection for discrete-time switched systems under dwell-time switching," *IEEE Transactions on Systems, Man, and Cybernetics: Systems*, vol. 50, pp. 3358-3368, 2020.
- [29] M. T. Raza, A. Q. Khan, G. Mustafa, and M. Abid, "Design of fault detection and isolation filter for switched control systems under asynchronous switching," *IEEE Transaction on control systems technology*, vol. 24, pp. 13-23, 2016.
- [30] Y. Eddoukali, A. Benzaouia, and M. Ouladsine, "Integrated fault detection and control design for continuous-time switched systems under asynchronous switching," *ISA Transaction*, vol. 84, pp. 12-19, 2019.
- [31] H. S. Nejad, A. R. Ghiasi, M. A. Badamchizadeh, and S. Pezeshki, " $H_\infty/H_-$  Simultaneous fault detection and control for continuous-time linear switched delay systems under asynchronous switching," *Transaction of the Institute of Measurement and Control*, vol. 41, pp. 263-275, 2019.
- [32] H. Azmi and A. Yazdizadeh, "Robust adaptive fault detection and diagnosis observer design for a class of nonlinear systems with uncertainty and unknown time-varying internal delay," *ISA Transaction*, 2022.
- [33] J. Huang, X. Hao, and X. Pan, "Asynchronous switching control of discrete-time linear system based on mode-dependent average dwell time," *International Journal of Control, Automation and Systems*, vol. 18, pp. 1705-1714, 2020.
- [34] A. Akhenak, M. Chadli, J. Ragot, and D. Maquin, "Fault detection and isolation using sliding mode observer for uncertain Takagi-Sugeno fuzzy model," *Proc. of the 16th Mediterranean Conference on Control and Automation*, pp. 286-291, 2021.
- [35] Y. Liu, X. Chen, J. Lu, and W. Gui, "Non-weighted  $l_2/L_2$  gain of asynchronously switched systems," *Nonlinear Analysis: Hybrid Systems*, vol. 43, 2021.
- [36] G. X. Zhong and G. H. Yang, "Asynchronous fault detection and robust control for switched systems with state reset strategy," *Journal of the Franklin Institute*, vol. 355, pp. 250-272, 2018.
- [37] S. Shi, Z. Shi, and Z. Fei, "Asynchronous control for switched systems by using persistent dwell time modeling," *Systems Control Letter*, vol. 133, 104523, 2019.
- [38] M. Chadli and M. Darouach, "Robust admissibility of uncertain switched singular systems," *International Journal of Control*, vol. 84, pp. 1587-1600, 2011.
- [39] F. Zhu, Y. Shan, and Y. Tang, "Actuator and sensor fault detection and isolation for uncertain switched nonlinear system based on sliding mode observers," *International Journal of Control, Automation and Systems*, vol. 19, pp. 3075-3086, 2021.
- [40] S. Shi, Z. Fei, and K. H. Reza, "Event-triggered control for switched T-S fuzzy systems with general asynchronism," *IEEE Transaction on Fuzzy Systems*, vol. 30, pp. 27-38, 2020.
- [41] S. Shi, Z. Fei, and M. Dai, "Asynchronously bounded filtering for discrete-time switched positive systems," *Nonlinear Analysis: Hybrid Systems*, vol. 44, pp. 101-121, 2022.
- [42] H. Habibi, I. Howard, S. Simani, and A. Fekih, "Decoupling adaptive sliding mode observer design for wind turbines subject to simultaneous faults in sensors and actuators," *IEEE/CAA Journal of Automatica Sinica*, vol. 8, pp. 837-847, 2021.
- [43] P. Huang, F. Qi, Y. Chai, and L. Chen, "Intermittent sensor faults detection based on fractional-order transient chaotic system," *IEEE Transaction on Instrumentation and Measurement*, vol. 71, 2020.
- [44] H. A. khani and N. Meskin, "Event-triggered robust fault diagnosis and control of linear Roesser systems: A unified framework," *Automatica*, vol. 128, 109575, 2021.
- [45] A. Akhenak, M. Chadli, D. Maquin, and J. Ragot, "Sliding mode multiple observer for fault detection and isolation," *Proc. of the 42nd IEEE International Conference on Decision and Control*, vol. 90, pp. 230-238, 2004.
- [46] J. Li, K. Pan, and Q. Su, "Sensor fault detection and estimation for switched power electronics systems based on sliding mode observer," *Applied Mathematics and Computation*, vol. 353, pp. 282-294, 2019.



**Shafqat Ali** received his B.E. degree in electronic engineering from Dawood University of Engineering and Technology Karachi, Pakistan and an M.Sc. degree in electrical engineering specialized in control systems from University of Engineering and Technology Lahore, Pakistan, in 2013 and 2017, respectively. Currently he is working toward a Ph.D. degree in control science and engineering from Harbin Institute of Technology Harbin, China. His research interests include robust control, fault diagnosis, switched systems, and sliding mode observer.



**Yuchen Jiang** received his B.E. degree in automation and a Ph.D. degree in control science and engineering from the Harbin Institute of Technology, Harbin, China, in 2016 and 2021, respectively. He is currently with the School of Astronautics, Harbin Institute of Technology. His research interests include data-driven process monitoring, fault diagnosis and prognosis, industrial cyber-physical systems, and artificial intelligence.

prognosis, industrial cyber-physical systems, and artificial intelligence.



**Hao Luo** received his B.E. degree in electrical engineering from Xi'an Jiaotong University, Xi'an, China, in 2007, and his M.Sc. and Ph.D. degrees in electrical engineering and information technology from the University of Duisburg-Essen, Duisburg, Germany, in 2012 and 2016, respectively. He is currently a Professor with the School of Astronautics, Harbin Institute

of Technology, Harbin, China. His research interests include model-based and data-driven fault diagnosis, fault-tolerant systems, and their plug-and-play application on industrial systems.



**Muhammad Taskeen Raza** received his B.Sc. and M.Sc. degrees in electrical engineering from the University of Engineering and Technology, Lahore, Pakistan, in 2004 and 2011, respectively, and a Ph.D. degree from the Department of Electrical Engineering, Pakistan Institute of Engineering and Applied Sciences, Islamabad, Pakistan, in 2016. He is currently working

as an Assistant Professor with the Department of Electrical Engineering, Lahore College for Women University (LCWU), Lahore. His current research interests include fault diagnosis, fault tolerant control, autonomous systems, system modeling, and system identification.



**Shah Faisal** received his B.E. (first-class Hons) and M.E. degrees in electrical power from the Sarhad University of Science and IT Peshawar, Pakistan, in 2012 and 2017, respectively. He is pursuing a doctoral degree in control science and engineering at the Harbin Institute of Technology in Harbin, China. His research interests include fault diagnosis in industrial processes, multi-agent systems, distributed control, and cyber-physical systems.

interests include fault diagnosis in industrial processes, multi-agent systems, distributed control, and cyber-physical systems.



**Faizan Shahid** received his B.S. degree in electronic engineering from Sir Syed University of Engineering and Technology Karachi, Pakistan and an M.S. degree in electrical engineering specialized in control systems from the National University of Science and Technology Karachi, Pakistan in 2011 and 2014, respectively. Currently, he is working toward a Ph.D. degree

in control science and engineering from Harbin Institute of Technology Harbin, China. His research interests include artificial intelligence, robust control, fault diagnosis, and optimization using neural network.

**Publisher's Note** Springer Nature remains neutral with regard to jurisdictional claims in published maps and institutional affiliations.